JOURNAL OF INFORMATION SCIENCE AND ENGINEERING 19, 857-879 (2003)

N-Sided Hole Filling and Vertex Blending Using Subdivision Surfaces*

WEI-CHUNG HWANG AND JUNG-HONG CHUANG
Department of Computer Science and Information Engineering
National Chiao Tung University
Hsinchu, 300 Taiwan

To fill an *N*-sided hole on a NURBS surface and to blend a corner formed by NURBS surfaces, we propose a regular *N*-sided open uniform quadratic subdivision surface derived by applying the open uniform quadratic subdivision scheme to a regular *N*-sided control mesh which is confined to the hole or to the region of the vertex blend. Boundary conditions such as C^0 and G^1-continuity required for the hole filling and vertex blending, are ensured by certain refinement steps performed in the course of the subdivision. The shape of the filling or blending surface is controlled by using fullness parameters. Methods are also proposed to represent the resulting regular *N*-sided open uniform quadratic subdivision surface using non-uniform rational B-spline surfaces.

Keywords: geometric modeling, subdivision surfaces, boundary control, *N*-sided hole filling, vertex blending

1. INTRODUCTION

N-sided hole filling and surface blending for both edges and corners are recurring operations in computer aided geometric design (CAGD). *N*-sided hole filling aims to provide surface patches that interpolate the hole's boundary curves, and needs also to satisfy smoothness conditions if the hole is a trimmed hole on a surface. Surface blending provides a smooth transition between adjacent base or primary surfaces so that sharp edges and corners can be rounded; see Fig. 1(a) for an illustration. The blend of two base surfaces is usually called *edge blend*, while the *vertex blend* is used to smoothly blend a corner formed by three or more base surfaces.

1.1 Previous Work

1.1.1 *N*-sided hole filling

Previously proposed methods for *N*-sided hole filling fall into two general approaches. The first approach fills a hole with rectangular patches by first splitting the hole into a rectangular mesh and then interpolating the mesh using a set of rectangular patches. The splitting is usually performed by connecting a center vertex of the hole to the middle point on each boundary curve. The bicubic Hermite patch is used in [1, 2] for the surface interpolation, while in [3] the rational Gregory patch is used. This approach may incur the

Received December 24, 2001; revised October 14, 2002; accepted December 12, 2002.
Communicated by Yung-Nien Sun.
* This work is supported by the National Science Council of the Republic of China under grant NSC 88-2213-E-009-061.

well-known *twist compatibility* problem [4], in which the twist vectors for patches around the center vertex are difficult to derive, especially when the number of incident edges is even.

The second approach fills the *N*-sided hole using a single patch. In [5, 6], the *N* incident edges, together with their cross tangents are blended with a blending function in a polygonal domain. In [7, 8], the polygonal patches are defined on non-planar domains. The use of non-planar domains introduces degrees of freedom which can be used in the construction of appropriate geometric continuity constraints between patches. The non-planar domain schemes have been shown to have difficulties when *N* is greater than six. In [9, 10], the *S-patch* is proposed to represent the *N*-sided patches. This method constructs a Berstein-Bézier polynomial defined on an $N - 1$ dimensional simplex. There still exist difficulties in practical applications when using this kind of representation for the *N*-sided patch. For example, the computation and evaluation of such representations are usually complicated, and it is hard to convert or exchange data between applications that have different *N*-sided patch representations.

1.1.2 Vertex blending

While many studies have been done on the edge blend [11-14], there are relatively few publications for the vertex blend due to its geometric and topological complexity [4, 6, 15-17]. The vertex blending for a corner formed by parametric surfaces is often derived by first blending the incident edges and filling the hole left around the corner. Positional and tangential continuity between the edge blend and each of the base surfaces must be satisfied along respective *linkage* or *contact curves*, on which the edge blend contacts the base surfaces. The same criteria must be satisfied between the vertex blend and base surfaces as well as incident edge blends.

As described in [4, 15], two different ways of the vertex blending have been proposed. The first, called *non-setback*, performs edge blends toward a corner until each pair of neighboring linkage curves meet, as shown in Fig. 1(a). The vertex blend becomes the filling of the *N*-sided hole bounded by *N* boundary cross sections of the incident edge blends (called the *profile curves*). Alternatively, a *setback* is specified for each edge to shrink the edge blend with the given setback distance from the corner; see Fig. 1 (b). Now we obtain a 2*N*-sided hole that is bounded by *N* profile curves as well as *N spring curves*, each of which lies on a base surface and connects the pair of neighboring profile curves lying on the base surface [4].

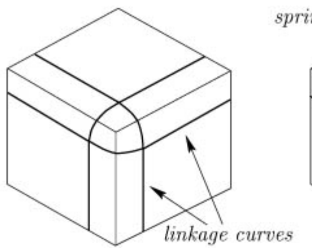

(a) Non-setback vertex blend.

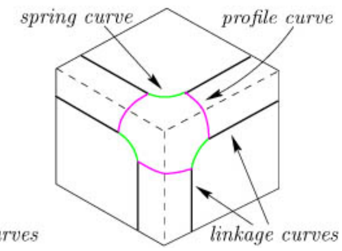

(b) Setback vertex blend.

Fig. 1. Non-setback and setback vertex blends.

As in the case of hole filling, the vertex blend can be represented by a single *N*-sided patch that interpolates the boundary curves and their relevant cross tangents. This representation is, however, not in a standard form. To represent the vertex blend using rectangular patches, most methods use the *center split* scheme that subdivides the hole by connecting a center point of the hole to the middle point of each profile and each spring curve (see Fig. 2(b)). The center split approach, however, often incurs the so called *twist compatibility* problem, as mentioned in section 1.1.1. A *setback split* scheme is proposed in [4] to circumvent the problem, by which the split interior regions usually have an add member of sides and there hence exists no twist incompatibility problem (see Fig. 2 (c)).

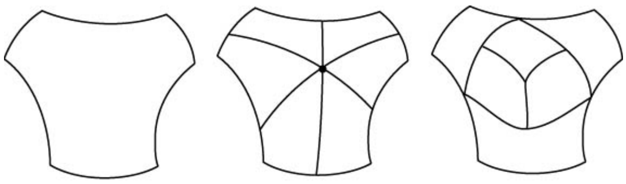

(a) *n*-sided patch (b) center split (c) setback split

Fig. 2. Methods to construct the vertex blend.

1.1.3 Subdivision surfaces and its boundary control

The subdivision surface, first introduced in [18, 19], is defined by recursively subdividing a mesh of arbitrary topology. At each step more vertices and smaller faces are created, and the subdivision surface is defined as the limit of the subdivision process.

Subdivision surfaces have recently been found to be useful in several areas, including reconstruction of unorganized 3D points [20], deformation [21], and character animation [22]. Before the subdivision surface become a popular representation in CAGD, however, methods that are able to control the shape and the boundary of the subdivision surfaces are highly desirable. In [23, 24] the boundary control of the quadratic subdivision surface is achieved by extending the control vertices along the boundary and the corner faces of the given mesh. The boundary control is, however, achieved only on the limiting subdivision surface. Although this allows us to control the C^0-continuity between adjacent limiting subdivision surfaces, its practical use in CAGD is still troublesome. In [25] a new open uniform quadratic subdivision scheme is proposed which is capable of achieving more effective boundary control, including C^0 and G^1-continuity at every subdivision step.

1.2 Overview

In this paper the open uniform subdivision scheme proposed in [25] is applied to a regular *N*-sided control mesh which is confined to the hole or to the region of the vertex blend. The boundary conditions, such as C^0 and G^1-continuity, required for hole filling and vertex blending are ensured by certain refinement steps performed in the course of the subdivision. The shape of the filling or blending surface can also be controlled by using fullness parameters.

In section 2 we propose regular *N*-sided open uniform quadratic subdivision surfaces which are especially designed for N-sided hole filling and vertex blending. With proposed open uniform quadratic subdivision surfaces, the interpolating schemes in [11, 26] for edge blending of parametric surfaces can be easily revised for construction of vertex blends. In sections 3 and 4 we detail how an N-sided hole on a parametric surface is filled and how a corner is blended by the regular N-sided open uniform quadratic subdivision surfaces, respectively. We then describe in section 5 how to represent and approximate the regular N-sided open uniform quadratic subdivision surface using non-uniform rational B-spline (NURBS) surfaces. Several implementation issues and examples are given in section 6. Section 7 gives some concluding remarks and future work.

2. REGULAR *N*-SIDED OPEN UNIFORM QUADRATIC SUBDIVISION SURFACE

2.1 Regular *N*-Sided Control Meshes

We first define a *regular N-sided control mesh of level m*, denoted RM_m^N, as the control mesh that has one N-sided face in the center, which is surrounded by N rectangular meshes G_m^0, G_m^1, and G_m^{N-1}, where G_m^i is an $m \times (m + 1)$ rectangular mesh of the following form

$$G_m^i = \begin{bmatrix} g_{00}^i & g_{01}^i & \cdots & g_{0m}^i \\ g_{10}^i & g_{11}^i & \cdots & g_{1m}^i \\ \vdots & \vdots & \cdots & \vdots \\ g_{(m-1)0}^i & g_{(m-1)1}^i & \cdots & g_{(m-1)m}^i \end{bmatrix}, \tag{1}$$

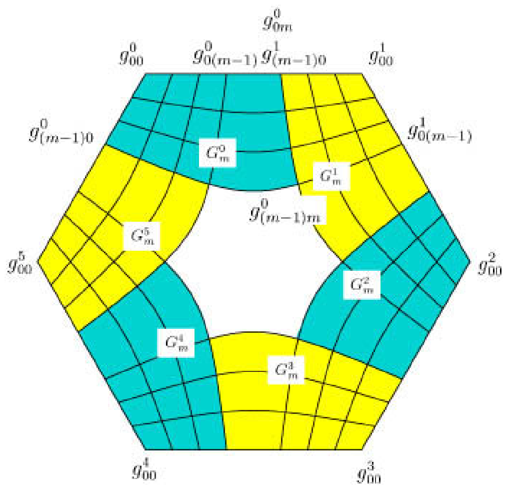

Fig. 3. A regular N-sided control mesh.

where the g^i_{jk} are control vertices; see Fig. 3. Each control mesh G^i_m is joined to one of its neighboring mesh $G^{(i+1)\bmod N}_m$ such that control vertices g^i_{jm} and $g^{(i+1)\bmod N}_{(m-1)j}$ are coincident for $j = 0, 1, \ldots, m-1$. The centered N-sided face is then defined by vertices $g^i_{(m-1)m}$, $i = 0, 1, \ldots, N-1$. Fig. 4 depicts examples of the regular N-sided control meshes RM^N_m for $N = 3, 5, 6, 9, 10$, and $m = 2, 3, 4, 8$. The meshes in the leftmost column are of level $m = 2$ and are the simplest regular N-sided control meshes, in which each G^i_m is a 2×3 control mesh.

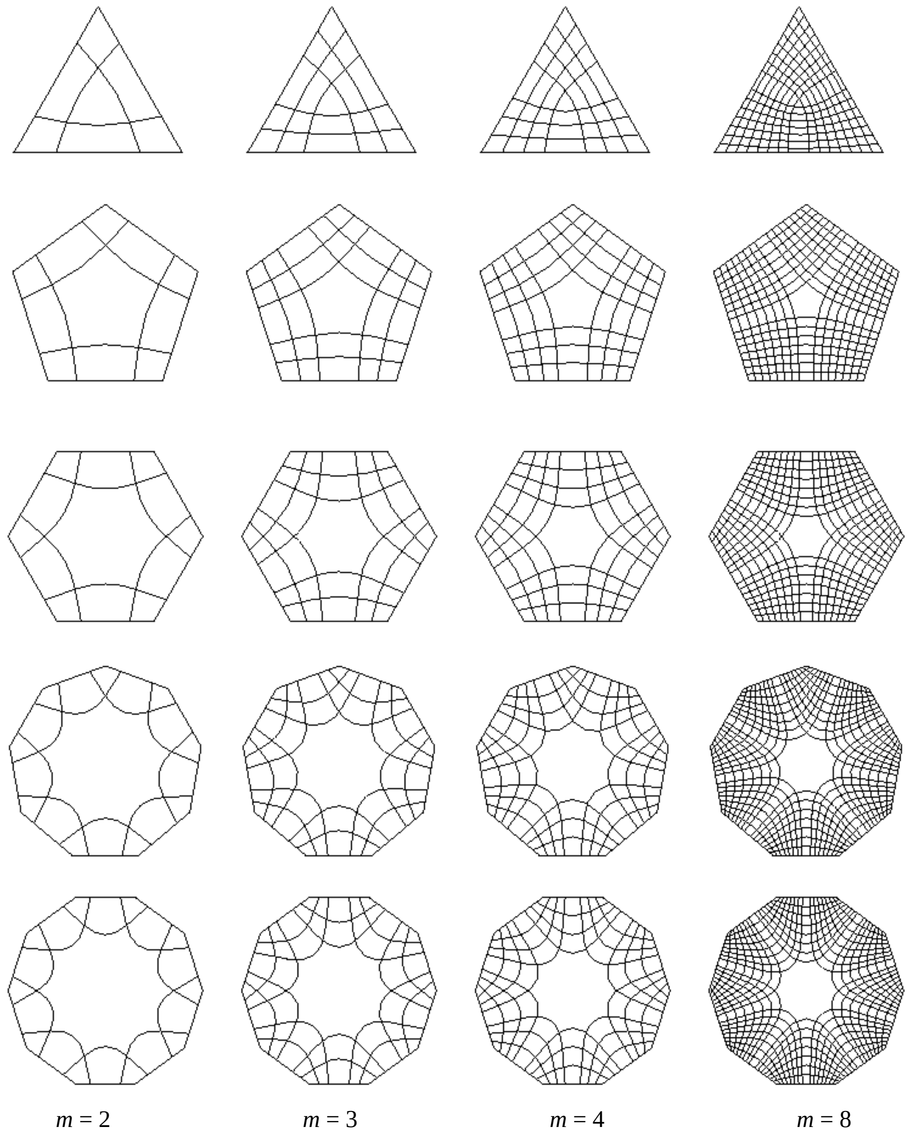

Fig. 4. Regular N-sided control meshes of different levels for $N = 3, 5, 6, 9$, and 10.

2.2 Open Uniform Quadratic Subdivision Scheme

The open uniform quadratic subdivision scheme described in [25] is proposed for control meshes of restricted topology. Note that, for a given regular N-sided control mesh RM_m^N, boundary and corner faces are all 4-sided. Moreover, all interior faces are 4-sided as well, except the centered face which is N-sided. According to [25] different subdivision weights are applied to corner, boundary, and interior faces as follows:

1. Given a 4-sided face F with four vertices P_{ij}, $P_{i(j+1)}$, $P_{(i+1)j}$, and $P_{(i+1)(j+1)}$, we have the following three types of subdivision:

   (a) Suppose F is a corner face in which P_{ij} is the corner vertex, $P_{(i+1)j}$ and $P_{i(j+1)}$ are two boundary vertices, and $P_{(i+1)(j+1)}$ is the interior vertex. The four new vertices after the subdivision are:

$$\begin{aligned} P'_{ij} &= P_{ij}, \\ P'_{(i+1)j} &= \frac{P_{ij} + P_{(i+1)j}}{2}, \\ P'_{i(j+1)} &= \frac{P_{ij} + P_{i(j+1)}}{2}, \\ P'_{(i+1)(j+1)} &= \frac{P_{ij} + P_{(i+1)j} + P_{i(j+1)} + P_{(i+1)(j+1)}}{4}. \end{aligned} \tag{2}$$

   (b) Suppose F is a boundary face in which P_{ij} and $P_{(i+1)j}$ are the boundary vertices, and $P_{i(j+1)}$ and $P_{(i+1)(j+1)}$ are the interior vertices. The four new vertices after the subdivision are

$$\begin{aligned} P'_{ij} &= \frac{3P_{ij} + P_{(i+1)j}}{4}, \\ P'_{(i+1)j} &= \frac{P_{ij} + 3P_{(i+1)j}}{4}, \\ P'_{(i+1)(j+1)} &= \frac{6P_{ij} + 2P_{(i+1)j} + 2P_{i(j+1)} + 6P_{(i+1)(j+1)}}{16}, \\ P'_{i(j+1)} &= \frac{2P_{ij} + 6P_{(i+1)j} + 6P_{i(j+1)} + 2P_{(i+1)(j+1)}}{16}. \end{aligned} \tag{3}$$

   (c) Suppose F is a 4-sided interior face. The four new vertices after the subdivision are

$$\begin{aligned} P'_{ij} &= \frac{9P_{ij} + 3P_{(i+1)j} + P_{i(j+1)} + 3P_{(i+1)(j+1)}}{16}, \\ P'_{(i+1)j} &= \frac{3P_{ij} + 9P_{(i+1)j} + 3P_{i(j+1)} + P_{(i+1)(j+1)}}{16}, \end{aligned} \tag{4}$$

$$P'_{(i+1)(j+1)} = \frac{3P_{ij} + P_{(i+1)j} + 3P_{i(j+1)} + 9P_{(i+1)(j+1)}}{16},$$
$$P'_{i(j+1)} = \frac{P_{ij} + 3P_{(i+1)j} + 9P_{i(j+1)} + 3P_{(i+1)(j+1)}}{16}.$$

which turns out to be the same as the quadratic subdivision scheme in [18, 19].

2. Suppose that the centered *N*-sided face is defined by vertices Q_j, $j = 0, 1, 2, \ldots, N-1$. After one step of subdivision, the new control vertex Q'_i corresponding to Q_i is defined as $Q'_i = \sum_{j=0}^{N-1} \alpha_{ij} Q_j$, where weights α_{ij} are computed in a similar manner as Eq. 4. We obtain the following weights

$$\begin{aligned} \alpha_{ij} &= (4N+2)/8N & |i-j| &= 0 \\ \alpha_{ij} &= (N+2)/8N & |i-j| &= 1 \\ \alpha_{ij} &= 2/8N & |i-j| &> 1, \end{aligned} \tag{5}$$

which is, again, the standard quadratic subdivision scheme described in [18, 19].

A regular *N*-sided control mesh remains as a regular *N*-sided control mesh after each step of the open uniform quadratic subdivision. In fact, for an initial regular *N*-sided control mesh of level *m*, a regular *N*-sided control mesh of level $(m-2) + 2^{j-1}$ is generated after the *j*-th subdivision step. When the open uniform quadratic subdivision scheme is applied to the regular *N*-sided control mesh, we denote the resulting limiting surface as the *regular N-sided open uniform quadratic subdivision surfaces*, or the *regular N-sided subdivision surface* for short.

2.3 Boundary Conditions of Regular *N*-sided Subdivision Surfaces

When the proposed regular *N*-sided subdivision surface is applied to fill an *N*-sided hole on a parametric surface, we require that the regular *N*-sided surface subdivision surface maintain C^0- and G^1-continuity to the trimmed surface. Thus we need to have a mechanism that is able to ensure C^0- and G^1-continuity, at least within a guaranteed tolerance. The boundary conditions achieved by the regular *N*-sided subdivision surface enable us to fulfill these goals; see [25].

To address the boundary conditions for the *i*-th boundary of the regular *N*-sided subdivision surface derived from a regular *N*-sided control mesh RM_m^N, we consider the following boundary rectangular control mesh

$$S_m^i = \begin{bmatrix} g_{00}^i & g_{01}^i & \cdots & g_{0m}^i & g_{(m-2)0}^{(i+1)\bmod N} & \cdots & g_{00}^{(i+1)\bmod N} \\ g_{10}^i & g_{11}^i & \cdots & g_{1m}^i & g_{(m-2)1}^{(i+1)\bmod N} & \cdots & g_{01}^{(i+1)\bmod N} \\ \vdots & \vdots & \cdots & \vdots & \vdots & \cdots & \vdots \\ g_{(m-1)0}^i & g_{(m-1)1}^i & \cdots & g_{(m-1)m}^i & g_{(m-2)(m-1)}^{(i+1)\bmod N} & \cdots & g_{(m-1)}^{(i+1)\bmod N} \end{bmatrix}, \tag{6}$$

where the first $m + 1$ columns are G_m^i of Eq. 1 and the last $m - 1$ columns form the transpose of the top-left $(m - 1) \times m$ submatrix of $G_m^{(i+1) \bmod N}$; that is, S_m^i represents the strip of all control vertices along the i-th boundary of RM_m^N; see Fig. 3. If we apply the open uniform subdivision scheme to S_m^i, we obtain a sub-patch of the regular N-sided subdivision surface which is the B-spline patch U_m^i defined by the rectangular control mesh S_m^i using the open knot vector $K_o^{2m+3} = [0001 \cdots (2m-3)(2m-2)(2m-2)(2m-2)]$ in the v direction and semi-open knot vector $K_s^{m+3} = [0001 \cdots m]$ in the u direction. The boundary conditions for the i-th boundary of the regular N-sided subdivision surface is identical to the boundary conditions of U_m^i as detailed in the following:

1. The i-th boundary curve of the regular N-sided subdivision surface is the open uniform B-spline curve defined by the control points $\{ g_{00}^i, g_{01}^i, \cdots, g_{0m}^i, g_{(m-2)0}^{(i+1) \bmod N}, \cdots, g_{00}^{(i+1) \bmod N} \}$ of RM_m^N and knot vector K_o^{2m+3}.
2. The cross tangent along the i-th boundary curve of the regular N-sided subdivision surface is the open uniform B-spline curve defined by control points $\{ g_{00}^i - g_{10}^i, g_{01}^i - g_{11}^i, \cdots, g_{0m}^i - g_{1m}^i, g_{(m-2)0}^{(i+1) \bmod N} - g_{(m-2)1}^{(i+1) \bmod N}, \cdots, g_{00}^{(i+1) \bmod N} - g_{01}^{(i+1) \bmod N} \}$ and knot vector K_o^{2m+3}.

With such boundary control mechanism the proposed regular N-sided subdivision surface can be used for N-sided hole filling and vertex blending, which is addressed in sections 3 and 4.

3. FILLING AN *N*-SIDED TRIMMED HOLE ON A PARAMETRIC SURFACE

Given an N-sided hole on an NURBS surface $P(s, t)$ (as shown in Fig. 5), we show how to fill the N-sided hole using the proposed regular N-sided subdivision surface. Moreover, the shape of the filling surface can be adjusted by assigning *fullness parameters* that are associated with corners of the subdivision surface. Suppose that the N-sided hole on $P(s, t)$ is specified by trimming curves $T_i(u)$, $i = 0, \ldots, N - 1$, defined on the (s, t)-domain. The regular N-sided subdivision surface will fill the hole and smoothly connect to $P(s, t)$ in the sense that C^0 and G^1-continuity along $T_i(u)$, $i = 0, \ldots, N - 1$, is within a pre-specified tolerance.

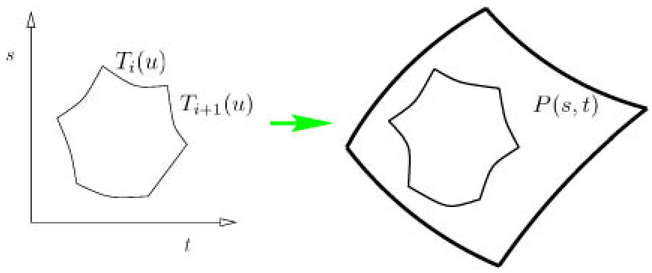

Fig. 5. An *N*-sided hole on a parametric surface.

To derive the N-sided filling subdivision surface, we first construct an initial regular N-sided control mesh that is of level 2 and confines to the trimming curves, then subdivide the mesh using the open uniform quadratic subdivision. In the meantime, after each step of subdivision the control mesh is refined so that the sampled boundary C^0 and G^1-continuity between $P(s, t)$ and the N-sided filling surface are ensured. The construction procedure consists of the following steps:

1. Construct an initial regular N-sided control mesh of level 2 and let $j = 2$.
2. Perform one step of the open uniform quadratic subdivision and do the following:

(a) For each boundary curve of the N-sided hole, we sample $2^j + 1$ data points and then refine the boundary faces of the regular N-sided control mesh according to the sampled data points.
(b) For each corresponding boundary curve of the N-sided hole and the current regular N-sided subdivision surface, we examine the C^0 and G^1-continuity error tolerances. If the error checking is satisfied for each boundary curve, we output the result and exit; otherwise set $j = j + 1$ and go to Step 2.

Next, we detail the computation in each step.

Step 1: To construct an initial N-sided control mesh of level 2, we first sample three vertices and one surface normal vector along each trimming curve of the N-sided hole. As a result, we obtain for each $T_i(u)$, $i = 0, \ldots, N - 1$, a set of three vertices $V_i = \{v_{i0}, v_{i1}, v_{i2}\}$ and a normal vector $\vec{n}_{i1}$ at v_{i1}, where $v_{i0} = P(T_i(0))$, $v_{i1} = P(T_i(0.5))$, and $v_{i2} = P(T_i(1.0))$.

Vertices in each V_i are then interpolated by a quadratic open uniform B-spline curve $C_i(u)$ using a uniform parametric interval. Suppose p_{i0}, p_{i1}, p_{i2}, and p_{i3} are four control points of $C_i(u)$. They are then used as the vertices on the i-th boundary of the initial regular N-sided control mesh; see Fig. 6(a). Note that the sampled vertex v_{i1} is at the middle of $\overline{p_{i1}p_{i2}}$ since the sampled vertices are interpolated using a uniform parametric intervals.

After deriving boundary vertices of the initial regular N-sided control mesh of level 2, we further derive the immediate interior vertices q_{i0}, $i = 0, \ldots, N - 1$. The cross tangent along the i-th boundary of the regular N-sided subdivision surface derived from this initial regular N-sided control mesh is an open uniform B-spline curve defined by the set of control points $\{p_{i0} - p_{(i+1)2}, p_{i1} - q_{i0}, p_{i2} - q_{(i-1)0}, p_{(i-1)0} - p_{(i-1)1}\}$. Thus the cross tangent of the subdivision surface at the middle of $\overline{p_{i1}p_{i2}}$ is

$$\vec{t}_i = \frac{q_{i0} + q_{(i-1)0}}{2} - \frac{p_{i1} + p_{i2}}{2} = \frac{q_{i0} + q_{(i-1)0}}{2} - v_{i1}.$$

To ensure G^1-continuity at the sampled vertex v_{i1} on the i-th boundary curve, $\vec{t}_i$ must lie on plane N_{i1} passing through vertex v_{i1} and orthogonal to sampled normal vector $\vec{n}_{i1}$. If we require that both q_{i0} and $q_{(i-1)0}$ lie on plane N_{i1}, then $\vec{t}_i$ will also lie on plane N_{i1}. That is, q_{i0} can be chosen from intersection line L_{i0} of plane N_{i1} and plane $N_{(i+1)1}$, where $N_{(i+1)1}$ is the plane passing through vertex $v_{(i+1)1}$ and orthogonal to surface normal $\vec{n}_{(i+1)1}$ at $v_{(i+1)1}$; see Fig. 6(b). Setting q_{i0} to be the projection of point p_{i0} onto line L_{i0} yields an N-sided filling subdivision surface with fullness parameter 0 at corner p_{i0}. In general, q_{i0} can be chosen according to a user-specified fullness parameter $f_i \geq 0$ using the following equation (see Fig. 6(c)):

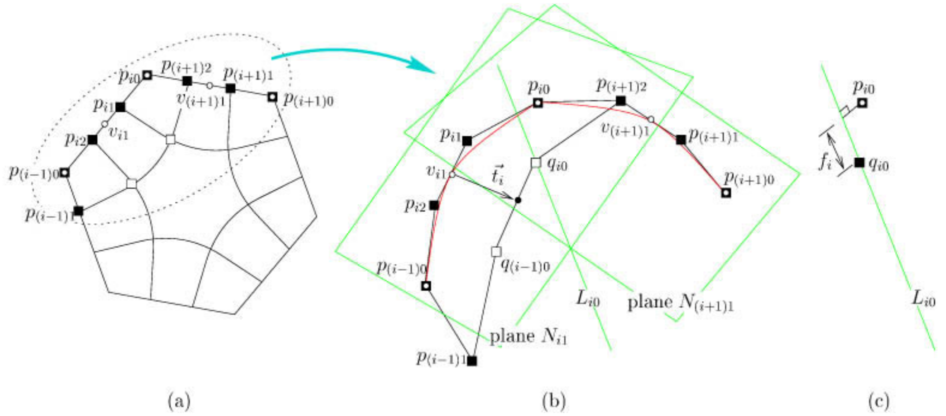

Fig. 6. The construction of an initial N-sided control mesh of level 3 in step 1.

$$q_{i0} = q_{i0}^{*} + f_i \vec{l}_{i0}, \tag{7}$$

where q_{i0}^{*} is the projection of p_{i0} onto L_{i0} and $\vec{l}_{i0}$ is the normalized tangent direction of line L_{i0}. Note that the q_{i0} obtained by Eq. 7 ensures that cross tangent $\vec{t}_i$ of the regular N-sided subdivision surface lies on plane N_{i1}, and hence the regular N-sided subdivision surface derived from the current regular N-sided control mesh will maintain G^1-continuity with $P(s, t)$ at the sampled vertex v_{i1}.

Step 2(a): Suppose we have performed the j-th step of open uniform subdivision. As a result, $2^j + 2$ new control vertices and new boundary faces are obtained along each boundary of the regular N-sided control mesh. To achieve a better C^0-continuity between $P(s, t)$ and the regular N-sided subdivision surface along a trimming curve, say $T_i(u)$, we next sample $2^j + 1$ vertices $v_{i0}, v_{i1}, \ldots$, and $v_{i(2^j)}$ uniformly on $T_i(u)$ and derive associated normal vectors $\vec{n}_{i1}, \vec{n}_{i2}, \cdots$, and $\vec{n}_{i(2^j-1)}$ at $v_{i1}, v_{i2}, \ldots$, and $v_{i(2^j-1)}$, respectively. Each set of vertices $V_i = \{v_{i0}, v_{i1}, \cdots, v_{i(2^j)}\}$ for the i-th boundary is then interpolated using uniform parameters $\{u_0, u_1, \cdots, u_{2^j}\}$ by a quadratic open uniform B-spline curve. The interpolation yields a curve $C_i(u)$ defined by $2^j + 2$ control points $\{p_{ik} \mid k = 0, \ldots, 2^j + 1\}$. We next replace those newly derived control vertices (the result of the j-th step of subdivision) on the i-th boundary of the regular N-sided control mesh by $p_{i0}, p_{i2}, \ldots, p_{i(2^j+1)}$; see Fig. 7(a). Such a replacement aims to improve the C^0-continuity between $P(s, t)$ and the regular N-sided subdivision surface.

Now, having derived a new set of boundary vertices, interior vertices q_{ik}, for $k = 0, 1, \ldots, 2^j - 1$, derived at j-th step of subdivision must be refined to ensure G^1-continuity (with bounded error) along trimming curve $T_i(u)$. That is, to achieve G^1-continuity along trimming curve $T_i(u)$, we refine q_{ik} to q'_{ik}, for $k = 0, 1, \ldots, 2^j - 1$. To obtain G^1-continuity at the sampled vertex v_{i1}, q_{i0} must lie on intersection line L_{i0} of the planes N_{i1} and $N_{(i+1)1}$, where N_{i1} is the plane passing vertex v_{i1} and orthogonal to surface normal $\vec{n}_{i1}$ at v_{i1}, and $N_{(i+1)1}$ is the plane passing vertex $v_{(i+1)1}$ and orthogonal to surface normal $\vec{n}_{(i+1)1}$ at $v_{(i+1)1}$. To do so, we project q_{i0} onto line L_{i0} to obtain q'_{i0}; as shown in Fig. 8(b). Other interior vertices q_{ik}, $k = 1, \cdots, (2^j - 1)$, are refined to new interior vertices q'_{ik} in a similar manner. Let plane N_{ik} be plane passing the vertex v_{ik} and orthogonal to $\vec{n}_{ik}$. The new interior vertices q'_{ik} must lie on both planes N_{ik} and $N_{i(k+1)}$ and is obtained by projecting q_{ik} onto intersection line L_{ik} of planes N_{ik} and $N_{i(k+1)}$; as depicted in Fig. 7(b).

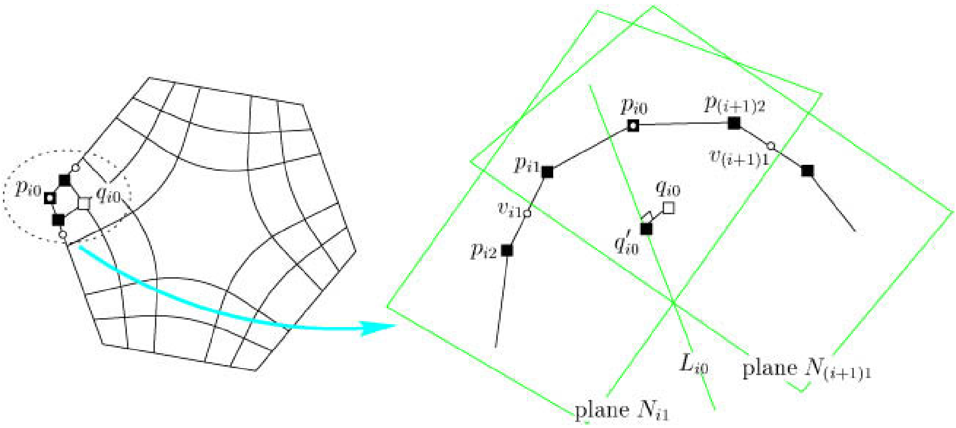

(a) (b)

Fig. 7. The refinement of corner interior vertex q_{i0} in step 2(a).

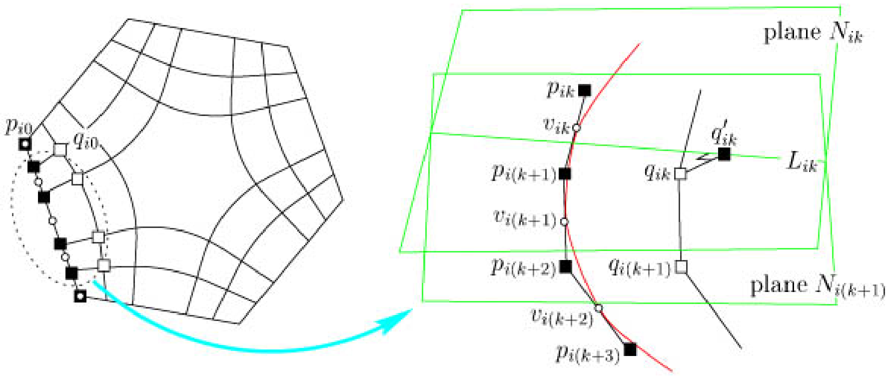

(a) (b)

Fig. 8. The refinement of other interior vertices q_{ik} in step 2(a).

Step 2(b): As a result of Step 2(a), the boundary curves of the regular *N*-sided subdivision surface is $C_i(u)$, which uniformly interpolates the sample points on corresponding boundary curves of the N-sided hole; that is, the interpolation occurs at the uniform parameter values $\{u_0, u_1, \ldots, u_{2^j+1}\}$ along boundary curves $T_i(u)$.

In step 2(b), the C^0 and G^1-continuity conditions of each mid-span between two adjacent parameter values are examined on each boundary curve. For each $C_i(u)$, we project points $c_{ik} = C_i((u_k + u_{k+1})/2)$, for $k = 0, \ldots, 2^j$, onto the NURBS surface $P(s, t)$ and obtain projection point c'_{ik} and normal vector $\vec{o}_{ik}$ at c'_{ik}. C^0-continuity at c_{ik} is ensured by checking whether the Euclidean distance between c_{ik} and c'_{ik} is smaller than a pre-specified tolerance $\in_d$, while G^1-continuity at c_{ik} is ensured by testing if the inner product of $\vec{o}_{ik}$ and $c_{ik} - d_{ik}$ is smaller than a specified tolerance $\in_n$. If the test succeeds for all sampled points on all boundary curves, we stop and output the current regular N-sided control mesh; otherwise we repeat Step 2. Note that the maximum error within a span $[u_k, u_{k+1}]$ does not usually occur at its midpoint. Nevertheless, reparameterization can in general move the maximum to the span's midpoint see for example [27].

4. VERTEX BLENDING OF PARAMETRIC SURFACES

The derivation of the regular N-sided subdivision surface for N-sided hole filling can be extended to vertex blend for either non-setback or setback paradigm, with one difference that here vertex blend can meet incident edge blends with C^1-continuity along the profile curves.

4.1 Non-setback Vertex Blending

For non-setback vertex blend, the boundary curves of the N-sided hole are the profile curves of the incident edge blends. Suppose we have N incident edge blends $G_i(s, t)$ and their associated profile curves $P_i(u)$ defined by

$$P_i(u) = G_i(s(u) = 1, t(u) = u),$$

for $i = 0, 1, \ldots, N - 1$; that is, $P_i(u)$ is the boundary cross section curve of the edge blend $G_i(s, t)$; see Fig. 9. The vertex blend can be derived by first filling the N-sided hole bounded by profile curves $P_i(u)$, $i = 0, 1, \ldots, N - 1$, using the procedure described in section 3. The hole filling procedure results in a regular N-sided subdivision surface of level m, for some $m \geq 2$, that has G^1-continuity to each incident edge blend at sampled points along the profile curve. Although the cross tangent of edge blends along the profile curve can be easily computed, ensuring C^1-continuity in the course of the hole filling process, however, may introduce conflict on cross tangent conditions derived from some pairs of neighboring edge blends. Hence, we first do the N-sided hole filling procedure and then, along each profile curve, adjust the cross tangent of the edge blend to be exactly the same as the corresponding cross tangent of the regular N-sided subdivision surface. That is, after the hole filling process, we perform one more derivation of edge blends in which the cross tangent conditions (in terms of control vertices) derived from the regular N-sided subdivision surface can be satisfied. Hence the edge blends and the regular N-sided subdivision surface can be joined exactly with C^1-continuity along each profile curve $P_i(u)$, $i = 0, 1, ..., N - 1$.

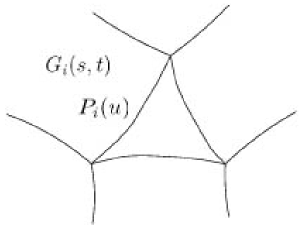

Fig. 9. Non-setback vertex blend.

4.2 Setback Vertex Blending

The boundary curves for the setback vertex blend for a corner are the profile curves of the incident edge blends as well as the spring curves that connect neighboring profile curves [4]. Suppose we have N edge blends incident to the corner. There will be N profile curves P_i together with N spring curves S_i, for $i = 0, \ldots, N-1$. One difference from the derivation of the non-setback vertex blend is that the interior vertices immediately adjacent to boundary vertices can be obtained according to the cross tangents of the edge blends without introducing any conflict.

Suppose profile curve P_i, for $i = 0, 2, \ldots, N-1$, is represented by an open uniform B-spline curve with four control points p_{i0}, p_{i1}, p_{i2}, and p_{i3}. The control points themselves are used as control vertices on the i-th boundary of the initial N-sided regular control mesh. To ensure exact C^1-continuity between edge blends $G_i(s, t)$ and the regular N-sided subdivision surface along profile curve P_i, interior vertices q_{i0} and $q_{(i+1)0}$ can be obtained directly using the cross tangents of $G_i(s, t)$ along P_i (see Fig. 10); that is,

$$q_{i0} = p_{i1} + \vec{t}_{i1} \text{ and } q_{(i+1)0} = p_{i2} + \vec{t}_{i2} \tag{8}$$

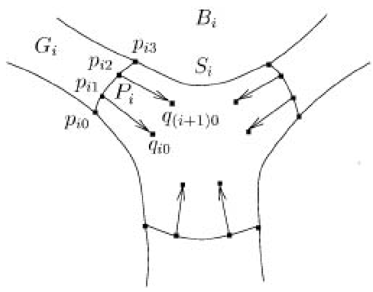

Fig. 10. Construction of a setback vertex blend.

where $\vec{t}_{i1}$ and $\vec{t}_{i2}$ are the cross tangents of the edge blend $G_i(s, t)$ at p_{i1} and p_{i2}, respectively. Note that since edge blend G_i and S_2^i (Eq. 6) of the initial regular N-sided control mesh have collinear cross tangents of the same magnitude, G_i and the surface represented by S_m^i of the regular N-sided control mesh of level m, for some $m \geq 2$, are joined with C^1-continuity; see [25]. As a consequence, the final regular N-sided subdivision surface is C^1-continuous with each incident edge blend along the profile curve. However, the continuity between the regular N-sided subdivision surface and each base surface is only approximate; i.e., it is only exact at only sampled points along the spring curve, like what we have seen for the N-sided hole filling.

5. REPRESSENTING THE REGULAR *N*-SIDED SUBDIVISION SURFACES USING NURBS SURFACES

The N-sided hole filling or vertex blending procedure results in a regular N-sided control mesh RM_m^N, for some level $m \geq 2$. Representing the regular N-sided subdivision surface derived from RM_m^N using NURBS surfaces is sometimes necessary since current CAD tools have no support for subdivision surfaces. One straightforward way is to represent the subdivision surface portion bounded by each rectangular mesh G_m^i of Eq. 1, $i = 0, 1, \ldots, N-1$, with a rectangular NURBS patch R_m^i using semi-open knot vector $K_s^{m+4} = [0\,0\,0\,1 \cdots (m+1)]$ in the v direction and $K_s^{m+3} = [0\,0\,0\,1 \cdots m]$ in the u direction, and to leave an N-sided hole in the center; as shown in Fig. 11(a). To ensure C^1-continuity between R_m^i and $R_m^{(i+1)\bmod N}$, for $i = 0, 1, \ldots, N-1$, each G_m^i is expanded to $G_m^{i\,\prime}$ by sharing the same boundary faces with $G_m^{(i+1)\bmod N}$ along their common boundary; that is,

$$G_m^{i\,\prime} = \begin{bmatrix} g_{00}^i & g_{01}^i & \cdots & g_{0m}^i & g_{(m-2)0}^{(i+1)\bmod N} \\ g_{10}^i & g_{11}^i & \cdots & g_{1m}^i & g_{(m-2)1}^{(i+1)\bmod N} \\ \vdots & \vdots & \cdots & \vdots & \vdots \\ g_{(m-1)0}^i & g_{(m-1)1}^i & \cdots & g_{(m-1)m}^i & g_{(m-2)(m-1)}^{(i+1)\bmod N} \end{bmatrix}. \tag{9}$$

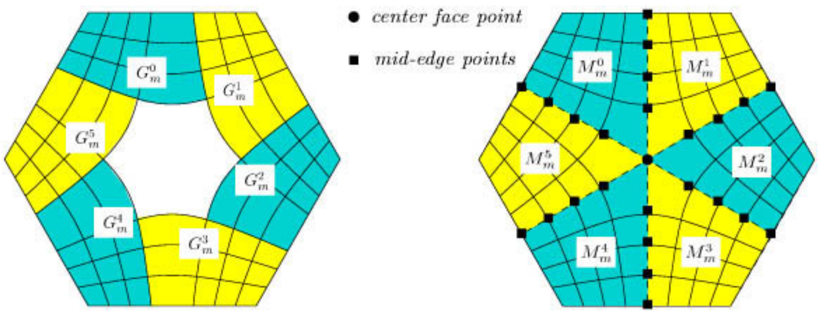

(a) Regular split method. (b) Mid-edge split method.

Fig. 11. Split of a regular N-sided quadratic subdivision surface.

Consequently, the B-spline patch $R_m^{i\,\prime}$ derived from $G_m^{i\,\prime}$ using semi-open knot vector $K_s^{m+5} = [0\,0\,0\,1 \ldots (m+2)]$ in the v direction and K_s^{m+3} in the u direction is thus smoothly joined with C^1-continuity to $R_m^{((i+1)\bmod N)'}$ derived from $G_m^{((i+1)\bmod N)'}$ using the same knot vectors. The regular N-sided subdivision surface can then be approximated by N B-spline patches $R_m^{0\,\prime}$, $R_m^{1\,\prime}$, $\cdots$, $R_m^{(N-1)\,\prime}$, together with the centered N-sided hole. We call such a method the *regular split method*.

Note that this representation will always leave an *N*-sided hole in the center. The area of the centered hole can be reduced by repeated application of the open uniform quadratic subdivision; that is, when we apply one step of the open uniform quadratic subdivision to the current mesh RM_m^N, we obtain a new regular *N*-sided control mesh of level $2(m-1)$, RM_{2m-1}^N; but with smaller center hole. Such an open uniform quadratic subdivision can be applied until the area of the center hole becomes smaller than a given tolerance. We then represent the regular *N*-sided subdivision surface with B-spline patches $R_l^{i\,\prime}$, $i = 0, \cdots, N-1$, for some $l > m$, and the centered polygon. We should note that such a repeated application of the open uniform subdivision on RM_m^N does not change the boundary continuity we obtained at the end of the hole filling and vertex blending process.

5.1 An Approximate NURBS Representation

We also propose a *mid-edge split method*, in which the regular *N*-sided control mesh is split into *N* rectangular meshes by adding a *center face point* c_m at the centroid of the center *N*-sided hole and *m mid-edge points* to be defined as follows. Given RM_m^N, a regular *N*-sided control mesh of level *m*, for each rectangular mesh G_m^i, we insert *m* mid-edge points d_{0m}^i, d_{1m}^i, … and $d_{(m-1)m}^i$, defined by

$$d_{km}^i = \frac{g_{k(m-1)}^i + g_{km}^i}{2}, k = 0,\ 1,\ \cdots,\ m-1;$$

see Fig. 12. Control mesh RM_M^N is then split into *N* rectangular meshes M_m^0, M_m^1, $\cdots$, and M_m^{N-1}, each of which shares with the adjacent mesh the inserted mid-edge points d_{0m}^i, d_{1m}^i, $\cdots$, and $d_{(m-1)m}^i$, and the center face point c_m; that is, the rectangular mesh M_m^i is defined by the following $m \times m$ matrix of vertices:

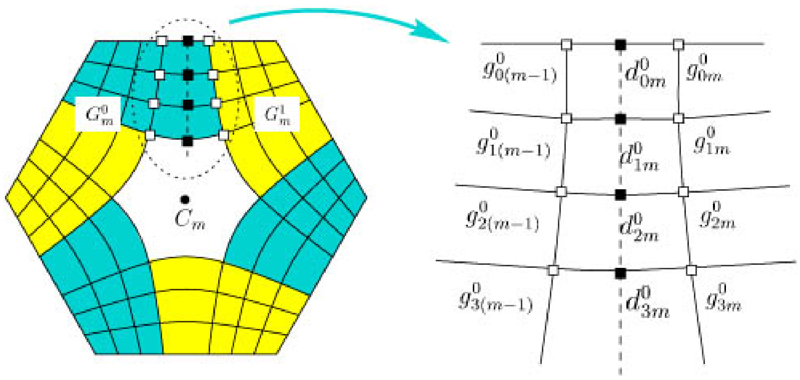

Fig. 12. Inserting the mid-edge point.

$$M_m^i = \begin{bmatrix} g_{00}^i & g_{01}^i & \cdots & g_{0(m-1)}^i & d_{0m}^i \\ g_{10}^i & g_{11}^i & \cdots & g_{1(m-1)}^i & d_{1m}^i \\ \vdots & \vdots & \cdots & \vdots & \vdots \\ g_{(m-1)0}^i & g_{(m-1)1}^i & \cdots & g_{(m-1)(m-1)}^i & d_{(m-1)m}^i \\ d_{0m}^{(i-1)\bmod N} & d_{1m}^{(i-1)\bmod N} & \cdots & d_{(m-1)m}^{(i-1)\bmod N} & c_m \end{bmatrix}; \tag{10}$$

see Fig. 11(b). The regular N-sided subdivision surface is then approximated by N B-spline surfaces B_m^0, B_m^1, $\cdots$, and B_m^{N-1}, where B_m^i is defined by the control array M_m^i using open uniform knots $K_0^{m+3} = [0001\cdots(m-3)(m-2)(m-2)(m-2)]$ in both directions. In the following, we claim that each patch B_m^i, for $i = 0, 1, \ldots, N-1$, is guaranteed to join its adjacent patches with C^1-continuity and lies on the regular N-sided subdivision surface derived from RM_m^N, except in the region of the center hole:

1. Since each B-spline patch B_m^i shares the same boundary vertices (the mid-edge points d_{km}^i, $k = 0, 1, \ldots, m-1$, and the center face point c_m) with patch $B_m^{(i+1)\bmod N}$, and both are derived using open uniform knots, they are exactly connected to each other with C^0-continuity.
2. Consider the following control mesh M_{ms}^i, which is obtained from M_m^i of Eq. 10 by removing the last row; that is,

$$M_{ms}^i = \begin{bmatrix} g_{00}^i & g_{01}^i & \cdots & g_{0(m-1)}^i & d_{0m}^i \\ g_{10}^i & g_{11}^i & \cdots & g_{1(m-1)}^i & d_{1m}^i \\ \vdots & \vdots & \cdots & \vdots & \vdots \\ g_{(m-1)0}^i & g_{(m-1)1}^i & \cdots & g_{(m-1)(m-1)}^i & d_{(m-1)m}^i \end{bmatrix}; \tag{11}$$

see Fig. 13 (a). Let B_{ms}^i be the B-spline patch derived from M_{ms}^i using open knot K_0^{m+4} = $[0001\cdots(m-2)(m-1)(m-1)\ (m-1)]$ in the v direction and semi-open knot K_s^{m+3} = $[0001\cdots m]$ in the u direction. Since we have $d_{km}^i = (g_{k(m-1)}^i + g_{km}^i)/2$, $k = 0, \cdots, m-1$, the two patches R_m^i and B_{ms}^i will have the same control mesh and knot vectors in both directions if knot refinement in the v direction is applied to B_{ms}^i. Thus, each sub-patch B_{ms}^i, $i = 0, 1, \cdots, N-1$, lies exactly on the regular N-sided subdivision surface.
3. Since the adjacent vertices between the two control meshes M_{ms}^i and $M_m^{(i+1)\bmod N}$ are collinear, and both patches use an open uniform knot along their common boundary, B_{ms}^i is joined to patch $B_m^{(i+1)\bmod N}$ with C^1-continuity.
4. Let M_{mp}^i be the control mesh derived from M_m^i by removing the last column; that is,

$$M_{mp}^i = \begin{bmatrix} g_{00}^i & g_{01}^i & \cdots & g_{0(m-1)}^i \\ g_{10}^i & g_{11}^i & \cdots & g_{1(m-1)}^i \\ \vdots & \vdots & \cdots & \vdots \\ g_{(m-1)0}^i & g_{(m-1)1}^i & \cdots & g_{(m-1)(m-1)}^i \\ d_{0m}^{(i-1)\bmod N} & d_{1m}^{(i-1)\bmod N} & \cdots & d_{(m-1)m}^{(i-1)\bmod N} \end{bmatrix}; \tag{12}$$

see Fig. 13(b). Let B_{mp}^i be the B-spline patch defined by M_{mp}^i using open knot K_o^{m+4} in the u direction and semi-open knot K_s^{m+3} in the v direction. Similar to the argument depicted in items 2 and 3, each B_{mp}^i also lies exactly on the regular N-sided subdivision surface and is joined to $B_m^{(i-1)\bmod N}$ with C^1-continuity.

From the above arguments, we conclude that each of the N split B-spline patches B_m^0, B_m^1, $\cdots$, and B_m^{N-1} lies exactly on the regular N-sided subdivision surface and smoothly joins its adjacent patches with C^1-continuity as well, except in the region that is

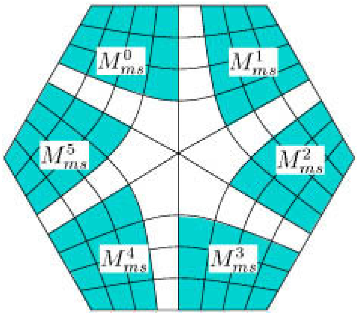

(a) Control meshes M^i_{ms}.

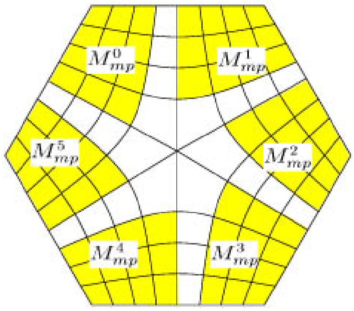

(b) Control mesh M^i_{mp}.

Fig. 13. Control meshes M^i_{ms} and M^i_{mp}.

not covered by both control meshes M^i_{ms} and M^i_{mp}, for $i = 0, 1, \ldots, N - 1$; i.e., except in the region of the center N-sided hole where only C^0-continuity is achieved. As previously stated, if we apply one step of the open uniform quadratic subdivision scheme to the regular N-sided control mesh RM^N_m, we obtain a new regular N-sided control mesh of level $2(m - 1)$, but with a smaller center N-sided hole. Such a subdivision can be applied until the area of the centered N-sided hole is smaller than a given tolerance. Fig. 14 shows a regular 6-sided subdivision surface that is the result of four subdivision iterations and is represented using the regular split method and mid-edge split method, respectively.

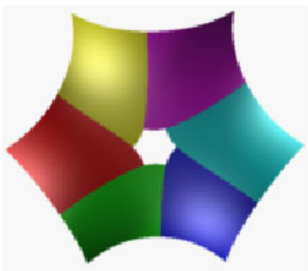

(a) Regular split method.

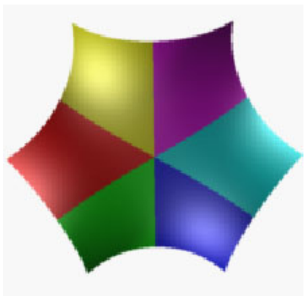

(b) Mid-edge split method.

Fig. 14. Splitting of a regular 6-sided subdivision surface.

6. EXAMPLES

The proposed method has been implemented on an SGI (with MIPS R5000/180MHZ CPU) as part of our *cggmlib* toolkit library in the *C* programming language. Fig. 15 shows the filling of a 5-sided hole on a B-spline surface using two different fullness parameters. Fig. 16 shows the setback vertex blends of a box's corner using two different fullness parameters. Fig. 17 shows the vertex blends for three intersecting planes having edge blends of mixed convexities. In Fig. 17(a) the setbacks of the convex edge blend are set to zero, and the vertex blending surface is 4-sided. In Fig. 17(b) the setback of the convex edge blend is non-zero, and the vertex blending surface becomes

6-sided. In Fig. 17(c), the fullness parameter corresponding to the convex edge blend is set to be larger than that for the other two concave edge blends. Fig. 18 shows the vertex blend of a box's corner where incident edge blends are all degenerated. Fig. 19 shows the non-setback vertex blend of a corner formed by six planes. Table 1 shows the number of subdivision steps required for C^0 and G^1-continuity tolerances of $\epsilon_d = 10^{-3}$ and $\epsilon_d = 10^{-2}$, respectively, and the time spent to construct the vertex blends. The proposed method is efficient since major computations involve only the evaluation of points, normal vectors of parametric surfaces, and the interpolation of data points.

Table 1. Statistics for constructing vertex blends.

Example	Fig. 16(b)	Fig. 17(b)	Fig. 18	Fig. 19
No. of subdivisions	3	3	4	3
Time in second	1.17	1.14	0.46	0.31

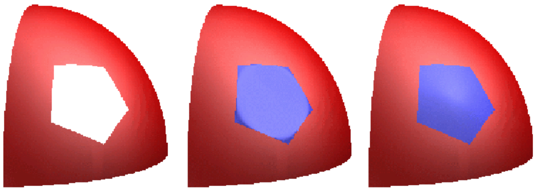

Fig. 15. Filling a 5-sided hole using fullness 0 (middle) and 1.0 (right).

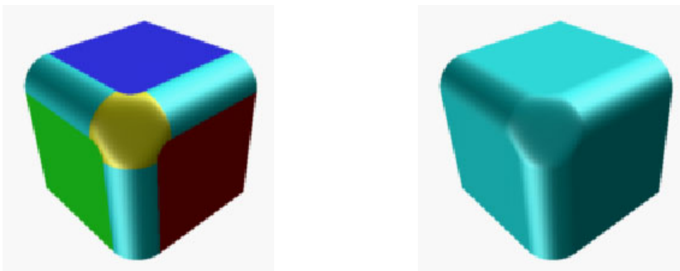

(a) With a smaller fullness parameter.

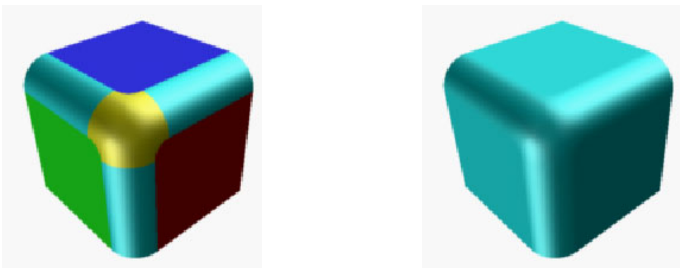

(b) With a larger fullness parameter.

Fig. 16. Setback vertex blends of a box's corner using different fullness parameters.

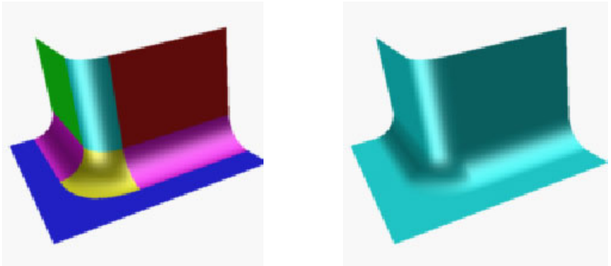

(a) Non-setback vertex blend.

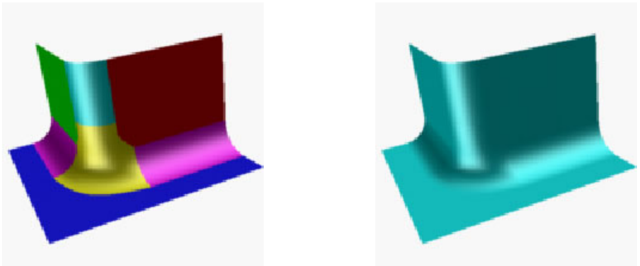

(b) Setback vertex blend.

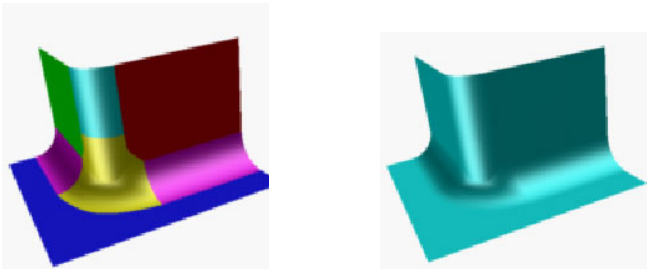

(c) With a larger fullness parameter for the convex edge blend.

Fig. 17. Vertex blends for three planes having edge blends of mixed convexities.

Experimental results show that our proposed methods are capable of constructing the vertex blend for corners having incident edge blends of mixed convexities and also provide some degree of flexibility in shape control using fullness parameters. The regular *N*-sided subdivision surface for all examples are finally converted into NURBS surface using the mid-edge split method. The area of the centered polygonal is usually small when the C^0 and G^1-continuity tolerances are satisfied. For the examples shown in 16(b) and 17(b), three steps of the subdivision are used to satisfy the C^0 and G^1-continuity for tolerances $\in_d = 10^{-3}$ and $\in_d = 10^{-2}$, respectively, and the ratio of the area ratio of the final center hole to the initial regular *N*-sided control mesh is 0.05631 and 0.07984 for examples shown in Figs. 16(b) and 17(b), respectively. The maximum G^1-continuity error between split NURBS patches in the region of the center hole is 0.000269 and 0.040511 for the examples shown in Figs. 16(b) and 17(b), respectively. These G^1-continuity errors are considered to be small enough for visual smoothness. Nevertheless, different from the area of the center hole, the maximum G^1-continuity error between split NURBS patches in the region of the centered hole is not guaranteed to converge to 0 when the subdivision of the regular N-sided mesh goes to infinitely many steps. Note that the maximum G^1-continuity error between NURBS patches resulting from the mid-edge split always occurs at the center split vertex since the difference of the cross tangents between two adjacent NURBS patches is defined by a quadratic B-spline curve in which the control points are all zero except at the center split vertex. Hence, the cross tangent difference is linearly increasing from 0 at $d^i_{(m-1)m}$, for $i = 0, 1, \ldots, N-1$, and reaches a maximum at the center split vertex c_m.

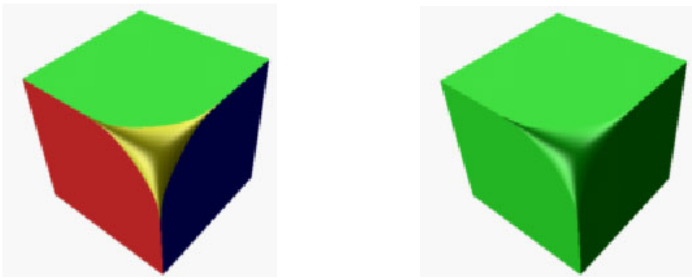

Fig. 18. A vertex blend of a box's corner having degenerated incident edge blends.

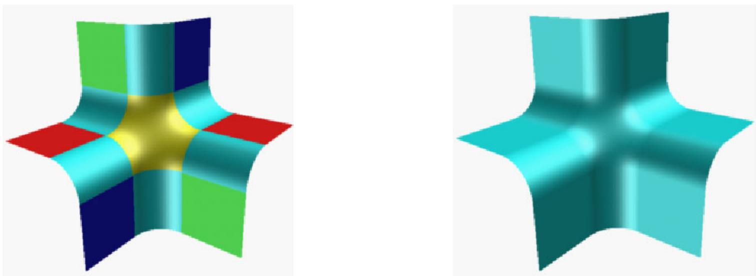

Fig. 19. Non-setback vertex blend of six planes having edge blends of mixed convexities.

7. CONCLUSIONS

We have proposed a regular N-sided open uniform quadratic subdivision surface to fill an N-sided hole on a parametric surface and to blend a corner formed by NURBS surfaces. The N-sided open uniform quadratic subdivision surface is derived by applying the open uniform quadratic subdivision proposed in [25] to an initial regular N-sided control mesh which confines to the hole or to the region of the vertex blend. The boundary conditions required for hole filling and vertex blend, including positional and tangential continuity, are obtained by some refinement steps guided by the boundary control mechanism possessed by the subdivision scheme. We have also proposed fullness parameter for the shape control on the regular N-sided open uniform quadratic subdivision surface. The resulting subdivision surface is itself an exact representation for the hole filling surface and the vertex blend. In order to incorporate the proposed methods to current CAD systems, however, the subdivision surface can either be represented hybridly by a set of NURBS surfaces and a centered *N*-sided hole, or solely by a set of NURBS surfaces that are exactly on the subdivision surface, except in the region of the centered *N*-sided hole where the subdivision surface is only approximated. However, in order to incorporate the proposed methods into current CAD systems, the subdivision surfaces can be represented in either of the following two ways:

1. by a set of NURBS surfaces and a center *N*-sided hole,
2. by a set of NURBS surfaces that are exactly on the subdivision surface.

In our current implementation, the tolerance value in section 3 still has to be manually adjusted. In the future, we will try to find better mechanisms to adjust the error tolerance, and improve the speed of the whole process. We are also currently investigating the convergence rate for the area of the center *N*-sided hole and an error measure for the NURBS approximation in the region of the centered hole.

REFERENCES

1. G. J. A. and J. Zhou, “Filling polygonal holes with bicubic patches,” *Computer Aided Geometric Design*, Vol. 11, 1994, pp. 391-410.
2. J. Hahn, “Filling polygonal holes with rectangular patches,” in W. Strasser and H. P. Seidel (eds.), *Theory and Practice of Geometric Modelling*, Springer Verlag, 1989, pp. 81-91.
3. H. Chiyokura, *Solid Modelling With DESIGNBASE*, Addison Wesley, 1988.
4. T. Varady and A. P. Rockwood, “Geometric construction for setback vertex blending,” *Computer Aided Design*, Vol. 29, 1997, pp. 413-425.
5. J. A. Gregory, V. K. H. Lau, and J. Zhou, “Smooth parametric surfaces and *N*-sided patches,” in M. Gasca and C. A. Miccheli (eds.), *Computation of Curves and Surfaces*, Kluwer Academic Publishers, 1990, pp. 457-498.
6. D. Plowman and P. Charrot, “A practical implementation of vertex blend surfaces using an N-sided patch,” in G. Mullineux (ed.), *Mathematics of Surfaces VI*, Oxford University Press, 1996.
7. M. Hosaka and F. Kimura, “Non-four-sided patch expression with control points,” *Computer Aided Geometric Design*, Vol. 1, 1984, pp. 75-86.
8. M. A. Sabin, “Non-rectangular surface patches suitable for inclusion in a B-spline surface,” in T. Hagen (ed.), *Proceedings of Eurographics*, 1983, pp. 57-69.
9. C. Loop and T. DeRose, “A multisided generalization of Bézier surfaces,” *ACM Transactions on Graphics*, Vol. 8, 1989, pp. 204-234.
10. C. Loop and T. DeRose, “Generalized B-spline surfaces of arbitrary topology,” *Computer Graphics*, Vol. 24, 1990, pp. 347-356.
11. J. H. Chuang and W. C. Hwang, “Variable-radius blending by constrained spine generation,” *The Visual Computer*, Vol. 13, 1997, pp. 316-329.
12. D. J. Filip, “Blending parametric surfaces,” *ACM Transactions on Graphics*, Vol. 8, 1989, pp. 164-173.

13. C. M. Hoffmann and J. Hopcroft, "The potential method for blending surfaces and corners," in G. Farin (ed.), *Geometric Modeling: Algorithms and New Trends*, SIAM Publications, USA, 1987, pp. 347-365.
14. J. Vida, R. R. Martin, and T. Varady, "A survey of blending methods that use parametric surfaces," *Computer Aided Design*, Vol. 26, 1994, pp. 341-365.
15. I. C. Braid, "Non-local blending of boundary models," *Computer Aided Design*, Vol. 29, 1997, pp. 89-100.
16. K. L. Hsu and D. M. Tsay, "Corner blending of free-form N-sided holes," *IEEE Computer Graphics & Applications*, Vol. 18, 1998, pp. 72-78.
17. M. Kosters, "Quadratic blending surfaces for complex corners," *The Visual Computer*, Vol. 5, 1989, pp. 134-146.
18. E. Catmull and J. Clark, "Recursively generated B-spline surfaces on arbitrary topological meshes," *Computer Aided Design*, Vol. 10, 1978, pp. 350-355.
19. S. Doo and M. Sabin, "Behaviour of recursive division surfaces near extraordinary points," *Computer Aided Design*, Vol. 10, 1978, pp. 356-360.
20. H. Hoppe, T. DeRose, T. Duchamp, M. Halstead, H. Jin, J. McDonald, J. Schweitzer, and W. Stuetzle, "Piecewise smooth surface reconstruction," in *Proceedings of SIGGRAPH* '94, 1994, pp. 295-302.
21. H. Qin, C. Mandal, and B. C. Vemuri, "Dynamic Catmull-clark subdivision surfaces," *IEEE Transactions on Visualization and Computer Graphics*, Vol. 4, 1998, pp. 215-229.
22. T. DeRose, M. Kass, and T. Truong, "Subdivision surfaces in character animation," in *Proceedings of SIGGRAPH* '98, 1998, pp. 85-94.
23. A. N. Nasri, "Polyhedral subdivision methods for free-form surfaces," *ACM Transactions on Graphics*, Vol. 6, 1987, pp. 29-73.
24. A. N. Nasri, "Boundary-corner control in recursive-subdivision surfaces," *Computer Aided Design*, Vol. 23, 1991, pp. 405-410.
25. W. C. Hwang, J. H. Chuang, and W. D. Hong, "Boundary control of subdivision surfaces using open uniform subdivision," in *Proceedings of 1998 Workshop on Computer Graphics*, 1998.
26. J. H. Chuang, C. H. Lin, and W. C. Hwang, "Variable-radius blending of parametric surfaces," *The Visual Computer*, Vol. 11, 1995, pp. 513-525.
27. P. C. Filkins, S. T. Tuohy, and N. M. Patrikalakis, "Computational methods for blending surface approximation," *Engineering with Computers*, Vol. 9, 1993, pp. 49-62.

Wei-Chung Hwang (黃維中) received a Ph.D. degree from National Chiao Tung University. He has been a member of the faculty at National Chiao Tung University. Dr. Hwang's research interests include computer graphics, geometric modeling, and network security. Currently, he is a researcher in Industrial Technology Research Institute.

Jung-Hong Chuang (莊榮宏) is a professor of computer science and information engineering department at National Chiao Tung University, Taiwan, R.O.C. His research interests include 3D computer graphics, virtual reality, and geometric modeling. Chuang received his B.S. degree in applied mathematics from National Chiao Tung University, Taiwan, in 1978, and M.S. and Ph.D. degrees in computer science from Purdue University in 1987 and 1990, respectively.